EMG-Based Model Predictive Control for Physical Human–Robot Interaction: Application for Assist-As-Needed Control

Tatsuya Teramae, Tomoyuki Noda, and Jun Morimoto

***Abstract*—In this letter, we propose an electromyography (EMG)-based optimal control framework to design physical human–robot interaction for rehabilitation and develop a novel assist-as-needed (AAN) controller based on a model predictive control (MPC) approach. To enhance the recovery of motor functions, encouraging the voluntary movements of patients is necessary while a therapist is assisting them. Therefore, in an AAN control framework, the robot only assists the deficient torque to generate a target movement. In our study, we first estimate the joint torque of a patient from measured EMG signals and then derive the deficient joint torque to generate the target movements by considering the patient's estimated joint torque with an MPC method. Results showed that our proposed method adaptively derived the necessary torque to follow the target elbow joint trajectories based on the subject's voluntary movements.**

***Index Terms*—Physical human-robot interaction, physically assistive devices, robust/adaptive control of robotic systems.**

I. Introduction

According to the World Health Organization, worldwide 15 million people annually suffer strokes [1]. Five million stroke survivors continue to suffer from permanent aftereffects [2], [3]. The annual cost of strokes has been estimated at 38 billion euros in Europe and 51 billion dollars in the USA [3], [4]. Therefore, the development of rehabilitation robots for stroke patients is attracting great attention [5].

In rehabilitation programs, active-assist exercise (AAE) is deemed a useful training method for stroke patients who can generate some movements without having sufficiently recovered to generate the target motions [6], [7]. Assist-as-needed (AAN) control is one way of implementing AAE using a robot system [8]. Previous studies showed that AAN control supports the recovery of stroke patients [8], [9].

We use an exoskeleton robot to enhance the recovery of stroke patients through an active-assist exercise framework. This management approach is called AAN control since a robot only supports a subject when additional assistance is necessary to conduct training motions [10]–[12]. Previously proposed AAN methods mainly used either a simple servo control approach or an adaptive control method. In servo control methods, the assistive robot simply increases the assistive torque based on the deviation of the current joint angle from the desired trajectory. Since even healthy humans have difficulty precisely tracking the desired trajectory, servo control is usually not applied if the tracking error is below a certain level, and so the assistive control system will not be too sensitive to small deviations from the desired trajectories due to natural human movement variations.

On the other hand, in the adaptive control approach, the movement parameters of a subject's limb are estimated so that the target motions can be precisely tracked with the estimated model parameters. Since the adaptive control approach, which has been used in a rehabilitation context [13], requires training trials to estimate the model parameters, a subject needs to move his own limb as well as the robot attached to it during the learning trials. Therefore, applying the adaptive control method to actual clinical situations is not straightforward.

Instead, we propose using electromyography (EMG) signals to estimate the subject's torque output. With EMG signals, we can estimate the torque output prior to the subject's actual movements. AAN control systems can consider the estimated torque output in the assistive controller design (Fig. 1). Actually, quite a few previous studies have been using EMG signals for joint torque estimation to control assistive robots or prosthetics [14], [15]. EMG signals have also been successfully used to train assistive robot movements with robot learning methods [14], [16].

In this study, we propose an EMG-based optimal control framework to design a novel AAN controller based on a model predictive control (MPC) approach. We first estimate the joint torque of a patient from the measured EMG signals and then derive the deficient joint torque to generate the target movements by considering the estimated patient's joint torque with an MPC method. Based on an online optimal controller design approach, we show that our proposed method adaptively derived the necessary torque to follow the target elbow joint trajectories while considering the subject's voluntary torque generation.

The rest of this letter is organized as follows. In Section II, we introduce related ANN studies. In Section III, we explain how

Manuscript received February 15, 2017; accepted July 12, 2017. Date of publication August 8, 2017; date of current version August 25, 2017. This letter was recommended for publication by Associate Editor G. Salvietti and Editor Y. Yokokohji upon evaluation of the reviewers' comments. This work was supported in part by the Commissioned Research of NICT and in part by SRPBS of AMED, "Research and Development of Advanced Medical Devices and Systems to Achieve the future of Medicine" from AMED, JSPS KAKENHI JP26820090, JP15H05321, JP16H06565, MIC-SCOPE 131207012, NEDO, ImPACT of CSTI. *(Corresponding author: Tatsuya Teramae.)*

The authors are with the Department of Brain Robot Interface, ATR Computational Neuroscience Laboratories, Kyoto 619-0288, Japan (e-mail: t-teramae@atr.jp; tomoyuki.noda@gmail.com; xmorimo@atr.jp).

Digital Object Identifier 10.1109/LRA.2017.2737478

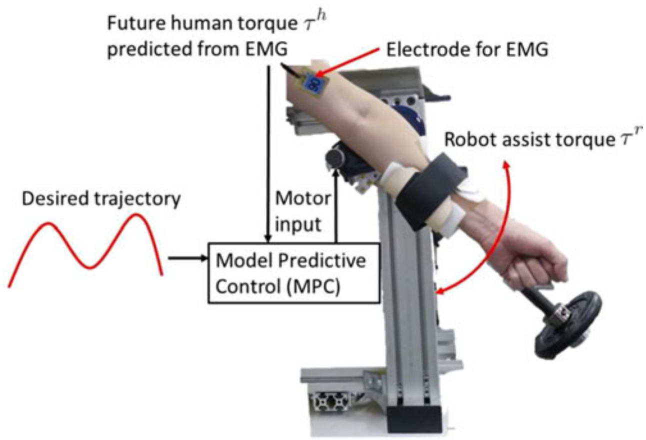

Fig. 1. Schematic diagram of proposed method: We estimate subject's torque prior to actual movement generation using surface EMG signals. Model predictive control (MPC) derives control input to track desired joint motion with estimated human joint torque. τ^r denotes robot torque, and τ^h denotes human torque.

we apply the MPC approach to ANN control. In Section IV, we introduce our elbow joint tracking task and explain how we evaluate our proposed method. In Section V, the results of the experiments are presented. Finally, in Section VI, we conclude this letter and discuss possible future studies.

II. Related Works

In this section, we briefly introduce how AAN strategies have been developed.

Even though implementing the servo control AAN approach is easy, generating assistive movements can still be useful based on the error between the desired trajectory and the user movement. Therefore, this approach has been widely used [17]–[19]. However, to properly track the desired trajectories, finding appropriate gain parameters is difficult, especially for patients since human body conditions are widely different. On the other hand, we cannot use very high-gain servo control for precise tracking because the assistive robots physically interact with human users. Therefore, high-gain servo control greatly inhibits the voluntary movements of subjects.

In the adaptive control approach, a user's movement model is identified through learning iterations. Since the assistive robot learns the necessary feedforward torque for movement assistance, servo gains can be small for tracking control systems. In a previous work [13], [20], radial basis functions (RBFs) flexibly represented the user movement model. However, the adaptive control approach's drawback is that such methods require learning iterations to identify the model parameters of the user movements. Thus, using adaptive control methods may not be very practical for clinical situations.

The difficulty of designing AAN controllers mainly comes from the unobserved user's torque output. Since it is not explicitly observed, we either need to use high-gain feedback as a conservative control strategy in the servo control approach or iterative learning trials to identify the motion model parameters in the adaptive control approaches. Therefore, the explicit extraction of torque output is very useful.

One possible approach to extract user's torque output is with a state estimation method [21]. Human joint torques were explicitly estimated using the Kalman filter in an AAN framework for a wrist joint assist control [22]. This previous AAN method used the difference between the actual state change and the state change estimated from the robot model to estimate the user torque input. Therefore, no additional measurement system was necessary for this framework. However, since it only uses the robot's joint state information and does not assume a user's movement model, it cannot be used for predicting the user's movements. Therefore, this kind of feedback-control-based approach requires careful gain parameter settings or several experimental trials for the gain tuning.

In our proposed method, we also considered user movements as external input to robot dynamics, but we used EMG signals to estimate the near future user's movements to optimize the robot controller based on the user torque output. Previous EMG-based robot control studies showed that EMG signals can predict user's torque output and the predicted results can generate robot behaviors [16]. In our study, we use the estimated user's joint torque as external input to the robot dynamics and solve an optimal control problem to derive an AAN controller. A model predictive control method is appropriate for taking the future user's torque output into account. We show that our robot can adaptively generate the necessary assistive torque based on the estimated user's torque output.

III. Method

A. Assist-As-Needed Control

The AAN approach assumes that users do their best to generate joint torques to track a target movement while deficient torques, which are necessary for precise tracking, are adaptively provided by an assistive robot to allow users to properly receive somatosensory inputs associated with successful tracking movements. The control input of the assist-as-needed (AAN) approach can be represented:

$$\tau^r = \tau^d - \tau^h, \tag{1}$$

where τ^r denotes the robot torque, τ^d denotes the desired torque to a track desired trajectory, and τ^h denotes the torque generated by the subject [22].

Fig. 1 shows a schematic diagram of our proposed method. In our EMG-based AAN framework, we estimated the subject's torque output τ^h prior to actual output from the measured EMG signals. Therefore, the model predictive control approach is suitable for explicitly taking the subject's torque output into account to precisely derive necessary additional joint torque τ^r to track the target rehabilitation movements. As a result, we expect that the robot only supports the subject's movements when additional torque input is necessary to track the target movements. If the user does not apply any torque, the controller still tries to track the trajectory. However, a critical point is that the users engage in generating the desired trajectory by themselves even if they can only generate a small amount of torque. In addition, even if the user's limb is moved by an exoskeleton robot, somatosensory inputs enhance the recovery of the nervous system [9].

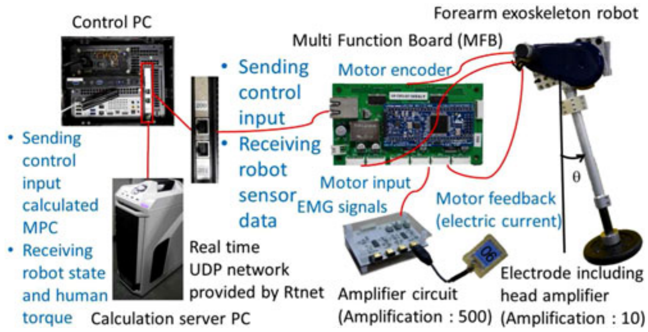

Fig. 2. Real-time control system of exoskeleton robot. Xenomai maintained real-time control loop. We developed a multi-function board (MFB) as I/O management system. Calculation server computes MPC control output. Control PC and MFB communicated by real-time UDP with RTnet. Control frequency was 200 Hz: Control PC (OS: Debian7 with Xenomai2.6.2, CPU: Intel (R) Core (TM) i5-3570K CPU @ 3.40 GHz, Memory: 16GB), Calculation sever PC (OS: Linux, CPU: Intel(R) Xeon(R) CPU E5-2697 v3 @ 2.60GHz, Memory: 64GB).

B. Controller Design

Fig. 2 shows our real-time control system. For the evaluation, we used our forearm exoskeleton robot that was actuated by a Maxon-geared EC motor with a gear ratio of $1:23$. Due to this low gear ratio, our exoskeleton robot's joint is backdrivable. Such backdrivability plays an important role in our AAN control framework. The robot's state was defined as θ and $\dot{\theta}$ are the robot's joint angle and its angular velocity. An inverse dynamics model of the exoskeleton robot in the continuous time domain can be given:

$$I\ddot{\theta} + h(\dot{\theta}) + g(\theta) = \tau^d, \tag{2}$$

where I represents the inertial parameter. The following is the friction term:

$$h(\dot{\theta}) = D\dot{\theta} + \Gamma_1 \tanh(\Gamma_2\dot{\theta}), \tag{3}$$

which is composed of viscous and static friction models. Γ_1 and Γ_2 are the static friction parameters, and $g(\theta)$ represents the gravity term. Then we estimate human joint torque $\hat{\tau}^h$ from the measured EMG signals (see Appendix A). By applying the estimated torque to (2), we have

$$I\ddot{\theta} + h(\dot{\theta}) + g(\theta) - \hat{\tau}^h = \tau^r. \tag{4}$$

We then derive optimal control input τ^r using MPC. In our AAN control method, the cost function for MPC is composed of the tracking error among the desired trajectory, the measured joint angle, and the robot control cost:

$$r_t = w_\theta(\theta_t - \theta_t^d)^2 + w_\tau(\tau_t^r)^2, \tag{5}$$

where θ^d denotes the desired joint angle at time t and w_θ and w_τ are the weight coefficients of the cost function. In our experiment, these cost function parameters were set to $w_\theta = 1.0 \times 10^6$ and $w_\tau = 0.1$. The prediction horizon was 0.2 s, which corresponds to $T = 40$ time steps since the control frequency was 200 Hz. This duration was determined based on the fact that EMG signals can be observed approximately 0.2 s prior to the actual human movements. Details of the MPC method are described in Appendix B.

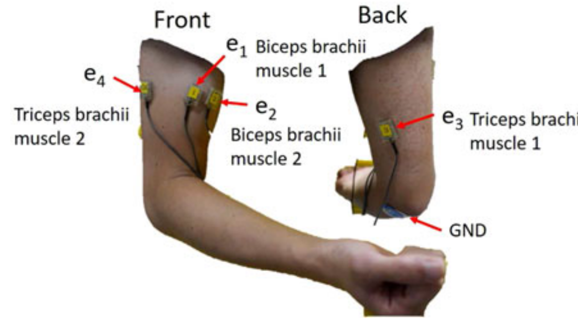

Fig. 3. EMG electrode placements: We put two EMG electrodes on the biceps (e_1 and e_2) and two on the triceps (e_3 and e_4).

IV. Experimental Setup

To evaluate our AAN method's control performance, we applied our proposed method to elbow joint tracking control tasks as target rehabilitation movements and also compared our proposed method with a non-EMG-based AAN approach [22].

A. EMG Measurements

We amplified the measured EMG signals ten times in the head amplifiers on the electrodes and then 500 times in the main amplifier. The amplified EMG signals were full-wave rectified and low-pass filtered with a cutoff frequency of 2.6 Hz.

In our experiments, we used the following four EMG electrodes to measure the muscle activities of the biceps and triceps:

$$\boldsymbol{e} = [e_1 \quad e_2 \quad e_3 \quad e_4]^\top. \tag{6}$$

The EMG electrode placements are depicted in Fig. 3. The torque estimation model depends on the EMG measurement condition and the properties of the user's body. Since the parameters need to be calibrated as in previous studies [13], [22], using a multi-user EMG interface approach [23] would be a useful future extension.

B. Elbow Joint Tracking Task

A curl exercise for the elbow joints is a standard rehabilitation training movement for stroke patients. We added a 0.5 kg weight at the tip of the robot to make the task difficult even for healthy subjects. This additional weight is not necessary for actual rehabilitation usage.

As the target movement profile, we considered a sinusoidal elbow joint trajectory with an amplitude of 20 deg and a frequency of 0.1 Hz for 10 seconds.

We determined the above task setups based on a previous work [22]. Our subject tracked the target trajectory by moving his elbow joint while looking at a monitor that displayed the target trajectory and his current joint angle (Fig. 4).

AAN control methods need to be able to support the limb movements of subjects by just assisting the additional torque that is necessary to track target movements. In this experiment, we aimed to show that our AAN controller can track the desired trajectory even when the user's voluntary contributions to generate the target movement were varied. We evaluated our method with the following three different conditions:

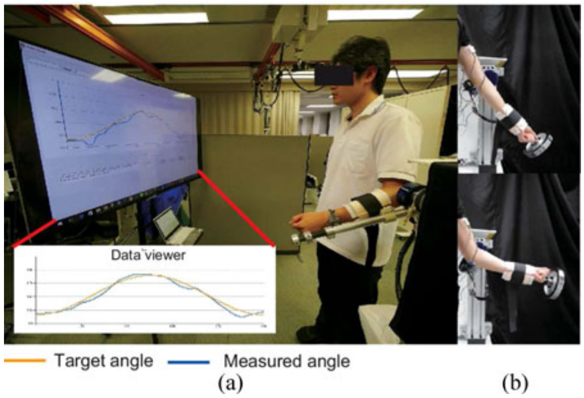

Fig. 4. Elbow joint tracking task: Subject's target movement and joint angle trajectory are presented on monitor.(a) Experimental setup and (b) Target movement.

1) Robot-dominant (RD) condition: The subjects relied on the exoskeleton robot to generate joint torque for the tracking task. The exoskeleton robot was expected to dominantly generate joint torque to track the target movements.
2) Robot-human cooperation (CO) condition: The subjects partially generated the necessary joint torque to collaboratively track the target trajectory with the exoskeleton robot.
3) Human-dominant (HD) condition: The subjects voluntarily generated joint torque to track the target movements. We expected that the exoskeleton robot would only generate a small amount of deficient torque for the target tracking.

We first conducted this elbow joint tracking task with one subject and asked him to do it five times to evaluate how the assistive torque can be adaptively changed based on the levels of his involvement in the given task.

To evaluate whether our proposed AAN framework works adequately for different users, we also conducted experiments in the RD and HD conditions with six subjects.

C. Comparison With Non-EMG-Based AAN method

Next we compare our proposed AAN framework with a state-of-the-art AAN method that does not use EMG signals to estimate the subject's torque output [22]. This non-EMG-based AAN approach was composed of two calculation steps. First, the human joint torque was estimated using a Kalman filter in which the error between the estimated and observed robot states was considered the result of the joint torque input generated by a human subject. Second, we derived the deficient torque, which is necessary to track the target trajectory, based on the estimated human joint torque in the first step. In this approach, a couple of parameters must be manually selected both in the first and second calculation steps. We experimentally selected appropriate parameters for these steps. Furthermore, we figured out different suitable gain parameter settings for RD and HD conditions.

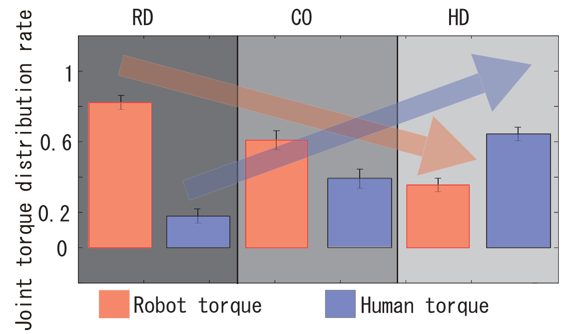

Fig. 5. Torque distribution in three different experimental conditions: robot-dominant (RD), robot-human cooperation (CO), and human-dominant (HD). Error bars represent standard deviation. According to increase of human subject involvement to target tracking task, joint torques were successfully reduced because this property is also desirable for AAN frameworks.

D. Comparison With Human Joint Control Without Robot Assistance

Next we compared the tracking performances with just human joint control to evaluate how the assistive joint torque generated by our proposed method helps generate large joint torque and precise movements.

We applied our proposed method to a periodic pattern that includes different frequencies since the target rehabilitation movements can be varied based on the capability of the patient's motor function. We considered a more complex tracking task than previous experimental setups: a target trajectory that includes three different sinusoidal bases with different frequencies of 0.5, 1.0, and 1.5 Hz, all of which were around the previous frequency range [22].

This experiment showed that our proposed method is even useful for a person who must accomplish a task that requires precise motions.

V. Results

A. Elbow Joint Tracking Performance With Three different Human Involvement Levels

Here we show the trajectory tracking performance and how the joint torque for the tracking task was generated.

Fig. 5 shows the torque distribution between the robot and a human subject in three different experimental conditions: robot-dominant (RD), robot-human cooperation (CO), and human-dominant (HD). The joint torque distribution rates of robot R_r and human subject R_h were derived as

$$R_r = \frac{\bar{\tau}^r}{\bar{\tau}^r + \bar{\tau}^h} \quad \text{and} \quad R_h = \frac{\bar{\tau}^h}{\bar{\tau}^r + \bar{\tau}^h}, \tag{7}$$

respectively, where $\bar{\tau} = \frac{1}{N}\sum_{t=1}^{N} |\tau_t|$ denotes an absolute average torque. We averaged the absolute torques over $N = 2000$ steps that corresponds to one experimental trial of 10 s. The error bars represent the standard deviation. According to the increase of the human subject's involvement in the target tracking task, the joint torques were successfully reduced. This property is desirable for an AAN framework.

In Fig. 6, we show the actual joint angle trajectories and the torque profiles of the robot and the human subject in the

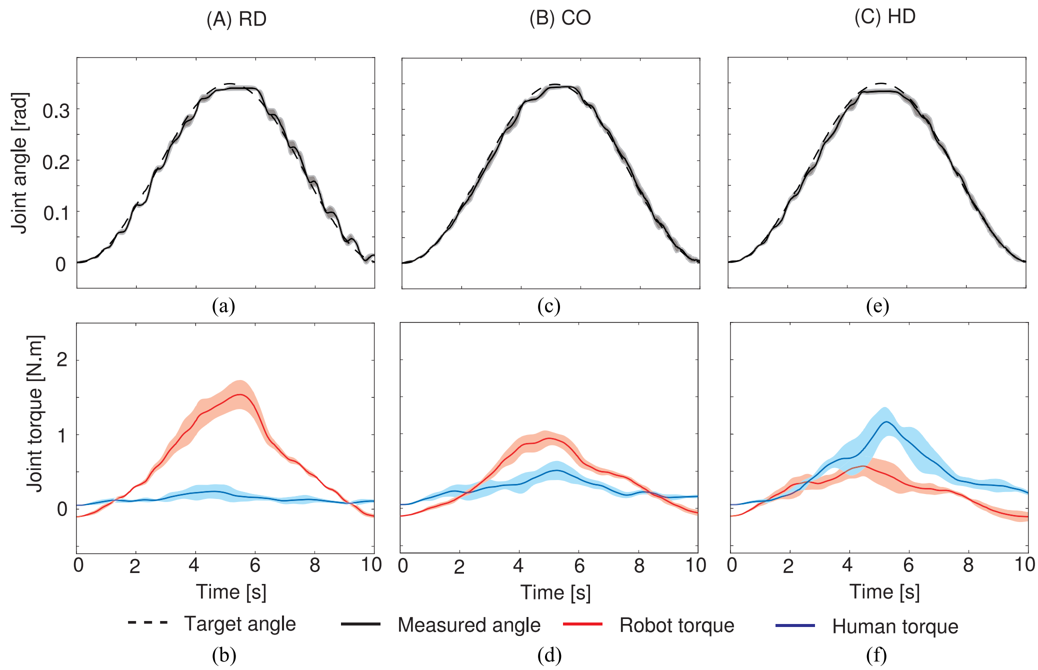

Fig. 6. Actual joint angle trajectories and torque profiles of robot and human subject in three different human involvement conditions. (a), (c), (e): With our proposed method, joint movements successfully followed target motion regardless of human involvement conditions. (b), (d), (f): According to three different human involvement levels, joint torque levels were adaptively modulated.

three different human involvement conditions. As seen in the top figures, with our proposed method, the joint movements successfully followed the target motion regardless of the human involvement conditions. On the other hand, according to the three different human involvement levels, as seen in the bottom figures, the joint torque levels were adaptively modulated.

We also evaluated our proposed method with six different subjects. The average torque distribution rate over the six subjects was $R_r = 0.94$, which equivalently means $R_h = 0.06$ with a standard deviation of 0.15 in the robot-dominant (RD) condition. In the human-dominant condition, the average torque distribution rate was $R_r = 0.26$, which equivalently means $R_h = 0.74$ with a standard deviation of 0.18. On the other hand, the average tracking error, e.g., root mean square error (RMSE), was 3.1×10^{-2} with a standard deviation of 8.0×10^{-3} in the RD condition. In the HD condition, the average tracking error was 1.5×10^{-2} with a standard deviation of 2.0×10^{-3}. In response to the human subject's involvement level, our proposed method accurately derived the deficient torque that was necessary to accomplish the tracking tasks even for different subjects.

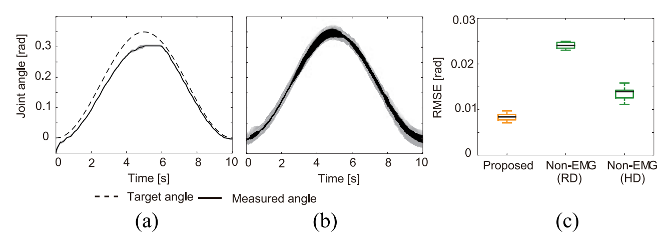

Fig. 7. Comparison with non-EMG-based method. (a) If we used HD gain parameter in RD condition for non-EMG-based method, tracking errors become much larger since larger gain is necessary in RD condition for accurate tracking. (b) If we used the RD gain parameter in the HD condition for non-EMG-based method, the tracking profiles become unstable due to the too large gain for the HD condition. (c) We compared average tracking errors of proposed and non-EMG-based methods. For our proposed method, we showed average performance over ten trials. For non-EMG-based method, we showed average tracking performances of the results presented in (a) and (b), where each condition includes five trials. Result show that average tracking error of the proposed method were significantly smaller than non-EMG-based method in two different conditions. Since our proposed method can predict subject's torque output before the actual motion, necessary torque can be more precisely and stably derived regardless of the human involvement conditions. Therefore, our method does not require careful gain tunings for different user's involvement levels.

B. Comparison With Non-EMG-Based AAN Method

We compared the assistive control performance of the proposed AAN method with the non-EMG-based AAN method in the RD and HD conditions. Drawback of the non-EMG-based approach is that it requires different appropriate gain parameter settings for different user's involvement levels. We first find suitable parameter settings for RD and HD conditions. If we used these gain parameters for corresponding conditions, the non-EMG-based method showed similar tracking performance to our proposed method. However, if we used the HD gain parameter in the RD condition, the tracking errors become much larger since larger gain is necessary in the RD condition for accurate tracking (Fig. 7(a)). On the other hand, if we used the RD gain parameter in the HD condition, the tracking profiles become unstable due to the too large gain for the HD condition (Fig. 7(b)).

In Fig. 7(c), we compared the average tracking errors of proposed and non-EMG-based methods. For our proposed method, we showed the average performance over ten trials. For the non-EMG-based method, we showed the average tracking performances of the results presented in Fig. 7(a) and (b), where

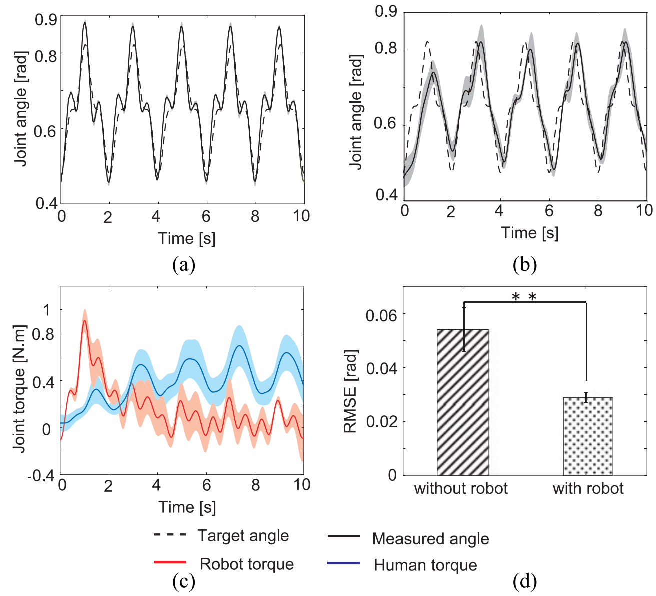

Fig. 8. Complex trajectory tracking task: (a) Tracking performance of proposed AAN method. Dashed line shows target trajectory, and solid line shows generated trajectory. Gray region represents area inside standard deviation although it is very small in this case. (b) Tracking performance of human subject. In this experimental setup, the robot did not generate any torque. Dashed line shows target trajectory, and solid line shows generated trajectory. Gray region represents area inside standard deviation. It was difficult for human subject to precisely track complex trajectory. (c) Generated joint torques by robot and human subject. Red line shows robot joint torque, and blue line shows estimated human joint torque. Subject dominantly generated joint torque by himself. Interestingly, for this complex movement, he initially relied on assistive robot torque and gradually generated target movement by himself. (d) Comparison of tracking errors between proposed method and pure human control without using robot. Exoskeleton robot with our AAN framework shows significantly better tracking performances.

each condition includes five trials. The result show that the average tracking error of the proposed method were significantly smaller than non-EMG-based method in the two different conditions. Since our proposed method can predict subject's torque output before the actual motion, necessary torque can be more precisely and stably derived regardless of the human involvement conditions. Therefore, our method dose not require careful gain tunings for different user's involvement levels.

C. Comparison With Only Human Control in Complex Trajectory Tracking Task

Finally, we evaluated our proposed method in a complex trajectory tracking task. In Fig. 8(a), we show the tracking performance of our proposed AAN method. The dashed line shows the target trajectory, and the solid line shows the generated trajectory. The gray region represents the area inside the standard deviation, although it is very small in this case. Our proposed method successfully worked even for a complex trajectory tracking task. In Fig. 8(b), we show the joint torques generated by the robot and the human subject. The red line shows the robot's joint torque, and the blue line shows the estimated human joint torque. The subject was instructed to voluntarily generate joint torque by himself. Interestingly, for this complex movement, he initially relied on the assistive robot torque and gradually generated the target movement by himself. Fig. 8(c) shows the tracking performance of the human subject. In this experimental setup, the robot did not generate any torque. The dashed line shows the target trajectory, and the solid line shows the generated trajectory. The gray region represents the area inside the standard deviation. The human subject had difficulty precisely tracking the complex trajectory. Fig. 8(d) compares the tracking errors between the proposed method and pure human control without using the robot. The exoskeleton robot with our AAN framework shows significantly better tracking performances. The above results indicate that our proposed method can also be useful in non-clinical situations.

VI. Discussion and Conclusion

In this study, we developed an assist-as-needed (AAN) controller design framework because estimating the deficient torque to accomplish a given task by considering the human user's contribution is the central issue of AAN controller design. The conventional approach uses a simple servo controller where the servo gain must be carefully selected. To improve the AAN control performance, adaptive control-based methods have been proposed. By estimating the user's movement model, task performances can be improved. However, iterative learning trials are necessary for this approach. If we can directly estimate the human user's torque output, the movement model estimation through an adaptive control approach may be obviated. In our approach, we used EMG signals to estimate the human torque output and derived exoskeleton robot control output with a model predictive control method that can take the estimated human torque output into account. Our proposed method successfully derived deficient joint torque based on the human users' involvement in the elbow joint tracking task. We also compared the proposed method with a non-EMG-based joint torque estimation method. Although our EMG-based method needed a measurement device to extract the torque output, we did predict how humans behave from the measured EMG signals. Therefore, our proposed AAN method showed more precise and stable tracking performance than the non-EMG-based approach regardless of the human involvement conditions. In addition, the subject reported that arm movements were more comfortably assisted by our proposed method than the non-EMG-based method. We finally evaluated it with a more complex trajectory tracking task and concluded that even in the human-dominant condition, our proposed AAN method is useful for precisely tracking target trajectories. This result indicates that the proposed method can also be useful for users those who do not have significant problems in their motor functions.

For the recovery of motor functions, the active participation of a user for generating a target rehabilitation movement is important [24]. Using high-gain servo control that prohibits the voluntary movements of users may not be a promising approach. On the other hand, if we use a relatively small gain for servo control, it is difficult for the robot to track the target movement due to the difficulty of gain tuning. Therefore, the tracking performance is one useful measure to evaluate the AAN control performance.

In our experiments with a limited movement duration, we did not observe the deterioration of the control performance due to muscle fatigue. However, for long-term training, online inference of the parameters of the torque estimation model in (8) is required.

Unlike the adaptive control approach based on the inverse dynamics model, we used optimal control under the forward dynamics constraint. Therefore, providing a target trajectory to the controller is not mandatory. For example, we can use more abstract targets such as target points to derive the AAN controller. In other words, the AAN task can be more flexible in our control framework.

An increase of joint stiffness due to spasticity is often observed. To cope with this problem, therapeutic electrical stimulation (TES) can be used [25]. Optimizing TES by measuring EMG signals is possible [26]. Therefore, the simultaneous optimization of TES and exoskeleton robot control is an interesting future research topic. In addition, future work will apply our method to control a multi-degree freedom lower-limb exoskeleton robot [27] for assisting biped locomotion.

Appendix

A. Joint Torque Estimation From EMG Signals

We preprocessed the measured EMG signals by full-wave rectification and low-pass filtering and used the processed EMG signals at time step t to estimate the joint torque at time step $t + k$. We considered a linear torque estimation model that has been frequently used in previous studies [15]:

$$\boldsymbol{\tau}^h_{t+k} = \boldsymbol{A}\boldsymbol{e}_t + \mathbf{b}, \tag{8}$$

where $\boldsymbol{A}$ and $\mathbf{b}$ are linear parameters. The EMG signals were observed approximately 0.2 seconds prior to the muscle tension force output [28]. Therefore, we set the prediction time step to $k = 40$ since the robot control frequency was 200 Hz.

We calibrated the linear parameters using the least-square estimation method with the squared error as follows:

$$E = \sum_t (\tau^h_t - \hat{\tau}^h_t)^2, \tag{9}$$

where τ^h_t is the human torque derived from the inverse dynamics model [21] and $\hat{\tau}^h_t$ is the estimated human torque derived from (8). Before each experiment, we calibrated the linear parameters. In the calibration process, subjects generated a sinusoidal movement twice, with and without a 0.5-kg weight on the tip of the robot. We used a total of 40 s of calibration data to find the linear parameters.

B. Model Predictive Control

We used the model predictive control (MPC) method to solve the optimal control problem to track the target movements based on the joint torque input estimated from the EMG signals. MPC is a model-based optimal control method in which such predicted future events as subject movements estimated by EMG signals can be explicitly taken into account. We derive T-step optimal control input sequence $\mathbf{u}_t, \ldots, \mathbf{u}_{t+T-1}$ from current time step t but only use first-step control input $\mathbf{u}_t$. At every control time step, T-step optimal control input sequences are derived for an objective function:

$$J = \min_{u_t, \ldots, u_{t+T-1}} \left[\Sigma_{k=t}^{T+t-1} r(\mathbf{x}_k, \mathbf{u}_k) + \Phi(\mathbf{x}_T) \right], \tag{10}$$

under dynamics constraint

$$\mathbf{x}_{t+1} = \mathbf{f}(\mathbf{x}_t) + \mathbf{g}(\mathbf{x}_t)\mathbf{u}_t, \tag{11}$$

where the state and control input were respectively defined as $\mathbf{x} = [\theta \quad \dot{\theta}]^\top$ and $u_t = \tau^r$. $\Phi(\mathbf{x}_T) = w_\theta(\theta_T - \theta^d_T)^2$ denotes the terminal cost.

Since we only use the first-step control output and recalculate the new optimal control problem at the next time step, MPC effectively works as a feedback control method, although each MPC calculation derives an open-loop control sequence. MPC methods have been applied to a system with such slow dynamics as chemical plants since MPC is computationally intensive. However, due to recent powerful computational resources, MPC is becoming a popular control approach even for robotic systems [29]–[32].

References

[1] J. Mackay et al., "The atlas of heart disease and stroke," Geneva, Switzerland: World Health Organization, 2004.

[2] C. Mathers, "The global burden of disease: 2004 update," Geneva, Switzerland: World Health Organization, 2008.

[3] S. Allender et al., "European cardiovascular disease statistics: 2008 edition," London: British Heart Foundation, 2008.

[4] A. L. Waldo et al., "Hospitalized patients with atrial fibrillation and a high risk of stroke are not being provided with adequate anticoagulation," *J. Amer. College Cardiology*, vol. 46, pp. 1729–1736, 2005.

[5] S. Hesse, H. Schmidt, C. Werner, and A. Bardeleben, "Upper and lower extremity robotic devices for rehabilitation and for studying motor control," *Current Opinion Neurology*, vol. 16, no. 6, pp. 705–710, 2003.

[6] J. L. Emken, R. Benitez, and D. J. Reinkensmeyer, "Human-robot cooperative movement training: Learning a novel sensory motor transformation during walking with robotic assistance-as-needed," *J. Neuroengineering Rehabil.*, vol. 4, no. 8, pp. 1–16, 2007.

[7] J. H. Carr and R. B. Shepherd, *Neurological Rehabilitation*. Gurgaon, India: Elsevier, 1998.

[8] P. S. Lum, C. G. Burgar, P. C. Shor, M. Majmundar, and M. V. der Loos, "Robot-assisted movement training compared with conventional therapy techniques for the rehabilitation of upper-limb motor function after stroke," *Arch. Phys. Med. Rehabil.*, vol. 83, no. 7, pp. 952–959, 2002.

[9] L. E. Kahn et al., "Robot-assisted reaching exercise promotes arm movement recovery in chronic hemiparetic stroke: A randomized controlled pilot study," *J. Neuroengineering Rehabil.*, vol. 3, no. 12, pp. 1–13, 2006.

[10] L. L. Cai, A. J. Fong, Y. Liang, J. Burdick, and V. R. Edgerton, "Assist-as-needed training paradigms for robotic rehabilitation of spinal cord injuries," in *Proc. 2006 IEEE Int. Conf. Robot. Autom.*, 2006, pp. 3504–3511.

[11] K. P. Michmizos and H. I. Krebs, "Assist-as-needed in lower extremity robotic therapy for children with cerebral palsy," in *Proc. 4th IEEE RAS/EMBS Int. Conf. Biomed. Robot. Biomechatronics*, 2012, pp. 1081–1086.

[12] F. Wang, D. E. Barkana, and N. Sarkar, "Impact of visual error augmentation when integrated with assist-as-needed training method in robot-assisted rehabilitation," *IEEE Trans. Neural Syst. Rehabil. Eng.*, vol. 18, no. 5, pp. 571–579, Oct. 2010.

[13] A. U. Pehlivan, F. Sergi, and M. K. O'Malley, "A subject-adaptive controller for wrist robotic rehabilitation," *IEEE/ASME Trans. Mechatronics*, vol. 20, no. 3, pp. 1338–1350, Jun. 2015.

[14] J. Rosen and M. Brand, "A myosignal-based powered exoskeleton system," *IEEE Trans. Syst., Man, Cybern., A, Syst. Humans*, vol. 31, no. 3, pp. 210–222, May 2001.

[15] K. Kiguchi and Y. Hayashi, “An EMG-based control for an upper-limb power-assist exoskeleton robot,” *IEEE Trans. Syst., Man, Cybern., B, Cybern.*, vol. 42, no. 4, pp. 1064–1071, Aug. 2012.

[16] L. Peternel, T. Noda, T. Petric, A. Ude, J. Morimoto, and J. Babic, “Adaptive control of exoskeleton robots for periodic assistive behaviours based on EMG feedback minimisation,” *PLoS One*, vol. 11, no. 2, pp. 1–26, 2016.

[17] C. Bower, H. Taheri, and E. Wolbrecht, “Adaptive control with state-dependent modeling of patient impairment for robotic movement therapy,” in *Proc. 2013 IEEE Int. Conf. Rehabil. Robot.*, 2013, pp. 1–17.

[18] H. I. Krebs *et al.*, “Rehabilitation robotics: Performance-based progressive robot-assisted therapy,” *Auton. Robots*, vol. 15, no. 1, pp. 7–20, Jul. 2003.

[19] G. D. Lee *et al.*, “Arm exoskeleton rehabilitation robot with assistive system for patient after stroke,” in *Proc. 12th Int. Conf. Control, Autom. Syst.*, 2012, pp. 1943–1948.

[20] E. T. Wolbrecht, V. Chan, D. J. Reinkensmeyer, and J. E. Bobrow, “Optimizing compliant, model-based robotic assistance to promote neurorehabilitation,” *IEEE Trans. Neural Syst. Rehabil. Eng.*, vol. 16, no. 3, pp. 286–297, Jun. 2008.

[21] J. Furukawa, T. Noda, T. Teramae, and J. Morimoto, “Estimating joint movements from observed EMG signals with multiple electrodes under sensor failure situations toward safe assistive robot control,” in *Proc. 2015 IEEE Int. Conf. Robot. Autom.*, 2015, pp. 4985–4991.

[22] A. U. Pehlivan, D. P. Losey, and M. K. O’Malley, “Minimal assist-as-needed controller for upper limb robotic rehabilitation,” *IEEE Trans. Robot.*, vol. 32, no. 1, pp. 113–124, Feb. 2016.

[23] T. Matsubara and J. Morimoto, “Bilinear modeling of EMG signals to extract user-independent features for multiuser myoelectric interface,” *IEEE Trans. Biomed. Eng.*, vol. 60, no. 8, pp. 2205–2213, Aug. 2013.

[24] K. Kawahira, M. Shimodozono, S. Etoh, K. Kamada, T. Noma, and N. Tanaka, “Effects of intensive repetition of a new facilitation technique on motor functional recovery of the hemiplegic upper limb and hand,” *Brain Injury*, vol. 24, no. 10, pp. 1202–1213, 2010.

[25] D. Kroon *et al.*, “Therapeutic electrical stimulation to improve motor control and functional abilities of the upper extremity after stroke: A systematic review,” *Clin. Rehabil.*, vol. 16, no. 4, pp. 350–360, 2002.

[26] Y. Muraoka, Y. Tomita, S. Honda, N. Tanaka, and Y. Okajima, “EMG-controlled hand opening system for hemiplegia,” in *Proc. 6th Vienna Int. Workshop Funct. Electrostimulation Basics Technol. Appl.*, 1998, pp. 255–258.

[27] B. Ugurlu *et al.*, “Variable ankle stiffness improves balance Control: Experiments on a bipedal exoskeleton,” *IEEE/ASME Trans. Mechatronics*, vol. 21, no. 1, pp. 79–87, Feb. 2016.

[28] D. A. Winter, *Biomechanics and Motor Control of Human Movement*, 2nd ed. Hoboken, NJ, USA: Wiley, 1990.

[29] E. Todorov and L. Weiwei, “A generalized iterative LQG method for locally-optimal feedback control of constrained nonlinear stochastic systems,” in *Proc. Amer. Control Conf.*, 2005.

[30] K. Ishihara and J. Morimoto, “Real-time model predictive control with two-step optimization based on singularly perturbed system,” in *Proc. 2015 IEEE-RAS 15th Int. Conf. Humanoid Robots*, 2015, pp. 173–180.

[31] K. Kanjanawanishkul and A. Zell, “Path following for an omnidirectional mobile robot based on model predictive control,” in *Proc. IEEE Int. Conf. Robot. Autom.*, 2009, pp. 3341–3346.

[32] M. Neunert, F. Farshidian, and J. Buchli, “Adaptive real-time nonlinear model predictive motion control,” in *Proc. IROS 2014 Workshop Mach. Learn. Plan. Control Robot Motion*, 2014, pp. 1–6.